Journal of Theoretical and Applied Physics (2020) 14:377–385
https://doi.org/10.1007/s40094-020-00394-1

RESEARCH

Comparative study of behavior of electrical conductivity in KI—Al_2O_3 and KI—TiO_2 heterostructure composites

Suhail Iqbal Wani[1] · Nazli Zeeshan[1] · Rafiuddin[1]

Received: 12 December 2019 / Accepted: 10 September 2020 / Published online: 28 September 2020

Abstract
The present work reports development of binary KI–Al_2O_3 and KI–TiO_2-based nanocomposites using simple solid-state reaction method and is characterized by X-ray diffraction, Fourier-transform infrared spectroscopy, scanning electron microscopy and impedance spectroscopy. The results show the effect of heterogeneously doped Al_2O_3 and TiO_2 on the ionic conductivity of pure KI which is moderately conductive. The results supported the composite development in which the interface layer portrays a significant part in governing the bulk properties of the compound. Improvement in electrical conductivity is seen in the incorporation of Al_2O_3 and TiO_2 dispersoid into the matrix of KI. With temperature, electrical conductivity increased and the activation energies were found to be decreasing. The activation energies for KI–Al_2O_3 and KI–TiO_2 systems were 0.22 eV and 0.21 eV, respectively, in the temperature range 20−400 °C. Dielectric constant increases with the increase in temperature in the entire temperature range studied attributed to the phenomenon of distortion of electric charges.

Keywords Solid composites · X-ray diffraction · Impedance spectroscopy · Ionic conductivity · Dielectric constant

Introduction

The modern world revolves around the portable electronic gadgets which store maximum energy in small units but provide better outcome. These devices bestow impetus in providing the enhanced ion conductivities. Since the last few decades, heterogeneous binary and tertiary composites are of main interest in the scientific world in manufacturing solid electrolyte composites which could provide electrochemical materials of higher qualities. These qualities may be improved ion conductivity or better photocatalytic activity [1–3]. A heterogeneous mixture of ionic salts and insulating chemically inactive materials forms a system called "ion-conducting composite'' which is considered as an advanced category of fast ion conductors or solid electrolytes, which plays an important part in improving the qualities of compounds, particularly at lower and modest temperatures. Space-charge areas usually occur close to prolonged defects (like surfaces and grain boundaries) in between two compounds in non-metallic phases [4].

Solid composite electrolyte forms a system which comprises of many phases (mainly two phases) in which many materials are combined to accomplish some acceptable material qualities like improvement in the ionic conductivity at room temperature. Mostly, the second phase comprises of non-conducting compounds such as TiO_2 and Al_2O_3, which are almost insoluble in the parent compound under normal circumstances [5, 6]. The enhancement in conductivity in the solid composite can be illustrated by the occurrence of a large number of extra source of point defects in the form of surfaces and interfaces [7]. The improvement in the ionic conductivity in multiphase composite systems is familiar for many years [8], but, only after 1973, the research interest in this field achieved excellence when Liang [9] stated nearly 50 times improvement in Li^+ ion conductor at room temperature merely by distributing nanoscale size particles of inert Al_2O_3 into the matrix of LiI. Afterward substantial amount of two-phase composite systems has been investigated with the conductivity improvement of approximately 1/3rd order of magnitude compared with those of component phases [10, 11]. Electrolytes comprised of two-phase composites were generally synthesized by distributing apparently micrometer size particles of insulating chemically inactive compounds

✉ Rafiuddin
rafiuddin.chem11@gmail.com

[1] Physical Chemistry Division, Department of Chemistry, Aligarh Muslim University, Aligarh 202002, Uttar Pradesh, India

(known as second-phase dispersoids) into a moderate-ion conducting components (known as first-phase host matrices). The conductivity improves with improved dispersoid concentration, reaches a peak value, and then decreases. The peak is normally intense, except for a few composite systems, like AgI–Al_2O_3 [12, 13].

Besides, the conductivity maxima vary with various solid composite systems and rely upon the composition of the second-phase chemically inactive dispersoid [14]. In composites of multiphase and polycrystalline materials interface plays an essential part for the ion transport properties. C. Wagner was the first person who explained the conductivity phenomena in the semiconducting two-phase metal oxide samples using the approach of space-charge layer [15], but the major attention on the theory of space-charge layer for the ionic conduction was brought by Liang in 1973 [9]. Wagner in 1989 played a major role in improving the conductivity in polyphase composite ceramics including the distribution of insulating nanoparticles in the matrix of ionic conductor and a mixture of two different ionic conductors [16]. Normally, the included oxides guide to acceptable mechanical properties and enrichment of ionic conductivity at room temperature [17–19]. The theoretical analysis of ionic conduction close to the interface was mostly done over by Mair in 1985 [20]. He gave a significant description of the conductivity enrichment established on the approach of the space-charge layer close to the phase boundary.

Potassium iodide salt comprises of well-structured fcc microcrystals [21] is broadly utilized to offer the iodide (I^-) ions required in the electrolyte [22, 23]. On comparing with smooth titanium dioxide (TiO_2) surface, TiO_2 with a suitable dopant, preferred texture, and/or porous structure with large surface area offers efficient hydrophilic properties. Recently, the potential of TiO_2 to improve its hydrophilicity has attracted researchers for various applications like smart coatings, surficial paintings/protectings, and biosensors [24]. In this work Al_2O_3 and TiO_2 have been used as insulating chemically inactive materials (second-phase dispersoids) into moderate-ion conducting KI solid (called first-phase host matrix) to study the behavior of ionic conductivity of KI–Al_2O_3 and KI–TiO_2 systems or to illustrate the effect of nanoparticles of Al_2O_3 and TiO_2 on the conducting behavior of KI. The influence of Al_2O_3 and TiO_2 particles and their effect on the physical, electrochemical, and dielectric properties of KI have been examined. The mole fraction 0.3 of KI has been taken the optimum concentration which resulted in the improved ion conductivity of KI. Hence, this work could lead the way that the moderate-ion conducting KI salt could be used as an electrochemical material.

Materials and methodology

Potassium iodide (KI) was used from Sigma-Aldrich with an established purity of 99.9%. Alumina (Al_2O_3) and titania (TiO_2) were taken from BDH Laboratory with an established purity of 99.9%. KI, Al_2O_3, and TiO_2 were separately ground for 2 h, blended with acetone followed by heating at 150 °C for 1 h to remove the moisture content. These materials were then ground again separately for an hour and filtered by using a sieve; 100−200 mesh particles of each material were taken. The appropriate amounts of Al_2O_3 and KI, and TiO_2 and KI were mixed intensively applying an agate motor and pestle to synthesize KI–Al_2O_3 and KI–TiO_2 composites. After that, these two amalgamations, (a) KI–Al_2O_3 and (b) KI–TiO_2 were kept in an electrical furnace at 300 °C for 5 h with occasional grinding for the initial reaction. The definite composite mixtures were grinding to finely powdered particles and placed in glasswares for further studies. Powder X-ray diffraction (XRD) performed by ''*Miniflex-II X-ray diffractometer Rigaku Corporation*" in the 2θ range from 10 to 80° with Cuka radiations confirmed the phase structure and crystal nature of composite materials. ''Perkin Elmer spectrum version 10.03.09" was used to carry out Fourier-transform infrared (FTIR) spectroscopic investigations in the range of 500–4000 cm^{-1} wave number at room temperature. Impedance analysis was executed with the help of a significant tester *Wayne Kerr-4300 LCR meter* in the frequency range 20 Hz–1 MHz at 50 °C, 200 °C, and 400 °C for round pellets pressed under 100 MPa pressures. The opposite surfaces of the round pellets were coated with carbon and annealed between the electrodes for 2 h at 200 °C to maintain enough electrical affinity between the samples and the electrodes. Scanning electron microscopy was carried out applying ''*Jeol−JSM 6510LV*'' and SEM images were taken for the powdered samples.

Result and discussions

XRD and FTIR analysis

Room-temperature X-ray powder diffraction (XRD) of the samples is displayed in Fig. 1; it predominantly depicts the cubic KI phase mixed with Al_2O_3 and TiO_2, respectively. The characteristic phase of KI was made certain by studying the predominant peaks as depicted in the XRD spectra in Fig. 1a. The single phase of KI shows the high symmetry cubic lattice structure (lattice parameter = 3.53 Å) according to PCPDF file no. 780750. The sharp crystalline peaks corresponding to KI salt are observed at $2\theta = 21.5°$,

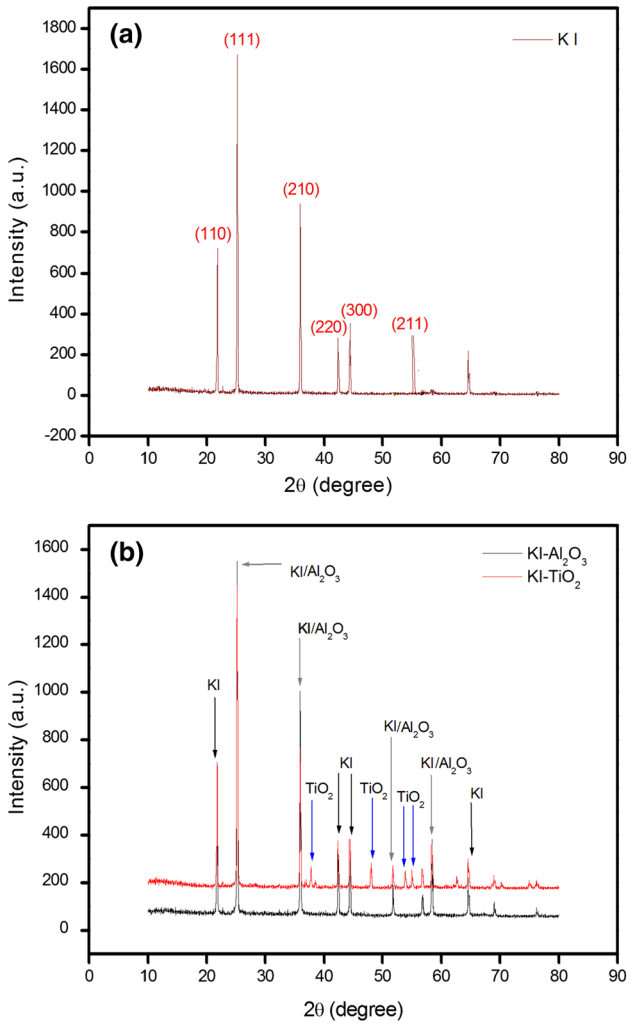

Fig. 1 X-ray diffractograms of **a** pure KI **b** KI–Al_2O_3 and KI–TiO_2 composites

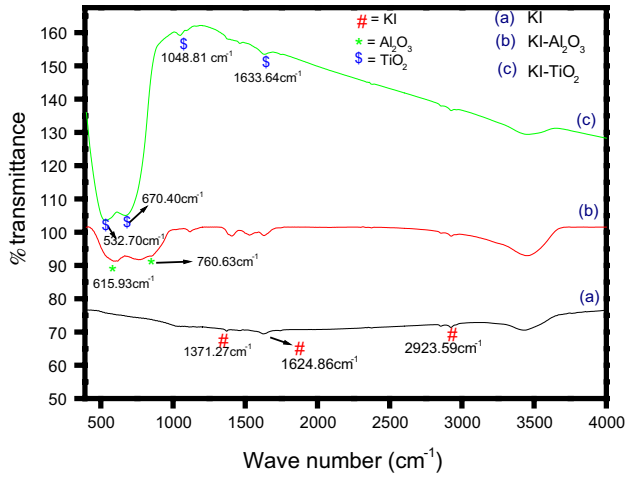

Fig. 2 FTIR spectra of pure KI and KI–Al_2O_3, and KI–TiO_2 composites

24.9°, 35.8°, 56.6°, and 64.4°, and corresponding crystal planes are mentioned in the figure. In a particular cubic fluorite type lattice, the substitution of a smaller cation by larger cation progressively decreases the lattice parameter. Here the lattice parameters change due to dissimilar ionic radii which cause to generate the lattice strain too. Because of the same crystal structure (cubic phase) of both KI and Al_2O_3, X-ray diffractions of KI doped with Al_2O_3 (JCPDS-ICDD file no. 46-1212) did not display any characteristic peak related to Al_2O_3. Such identical investigations were also seen in TlI–Al_2O_3, CsI–Al_2O_3 solid electrolyte systems [6, 25]. But in the matter of KI doped with TiO_2 additional peaks peculiar to TiO_2 anatase phase (JCPDS file no. 21-1272) were detected with characteristic 2θ values at 37.3°, 47.6°, 53.5°, and 55.1° these correspond to (004), (200), (105), and (211) crystal planes [26, 27]. However, if TiO_2 is calcined at substantial temperature or mixed with other impurities, anatase phase could transfer to the rutile phase [28].

FTIR spectra for pure KI and composite samples (KI−Al_2O_3 and KI−TiO_2) are depicted in Fig. 2. In the spectrum of the sample (a) the characteristic bands of KI salt were observed at 1371.27 cm^{-1}, 1624.86 cm^{-1}, and 2923.59 cm^{-1} [29]. Some additional peaks were visible in the spectra of samples (b) and (c) which confirms the formation of the composite. The spectra (b) depict peaks at 615.93 cm^{-1} and 760.63 cm^{-1} which attributed to Al-O vibrations of γ-Al_2O_3 [30]. The bands in the sample (c) at 532.70 $cm^{-1}$and 670.40 cm^{-1} correspond to the Ti–O stretching vibrations while the peak seen at 1048.81 cm^{-1} ascribed to Ti–O bending vibrations. The stretching vibrations of Ti–O-Ti were indicated by the peak at 1633.64 cm^{-1} [31]. Broad bands in all the samples around 3431.84 cm^{-1} and 3454.08 cm^{-1} were due to stretching vibrations of the O–H bonds of water molecules [32].

Scanning electron microscopy

Figure 3a–c represents the SEM micrographs of pure KI, KI−Al_2O_3, and KI−TiO_2 composites, respectively. The SEM micrographs are for the mixture containing 0.3 mol fraction of Al_2O_3 and TiO_2. It illustrates the incorporation of Al_2O_3 and TiO_2 particles into the matrix of a large average-sized KI particles. This arrangement of Al_2O_3 and TiO_2 particles in between the grain particles of ionic salt (KI) is supported by the local thermodynamic equilibrium owing to the wetting of Al_2O_3 and TiO_2 particles by KI grain particles during the formation of the amalgam [33]. Such kind of arrangement is of great importance in creating a large number of point defects in the form of surfaces. This distinct area between the ionic salt (host matrix) and the added oxide (dispersoid)

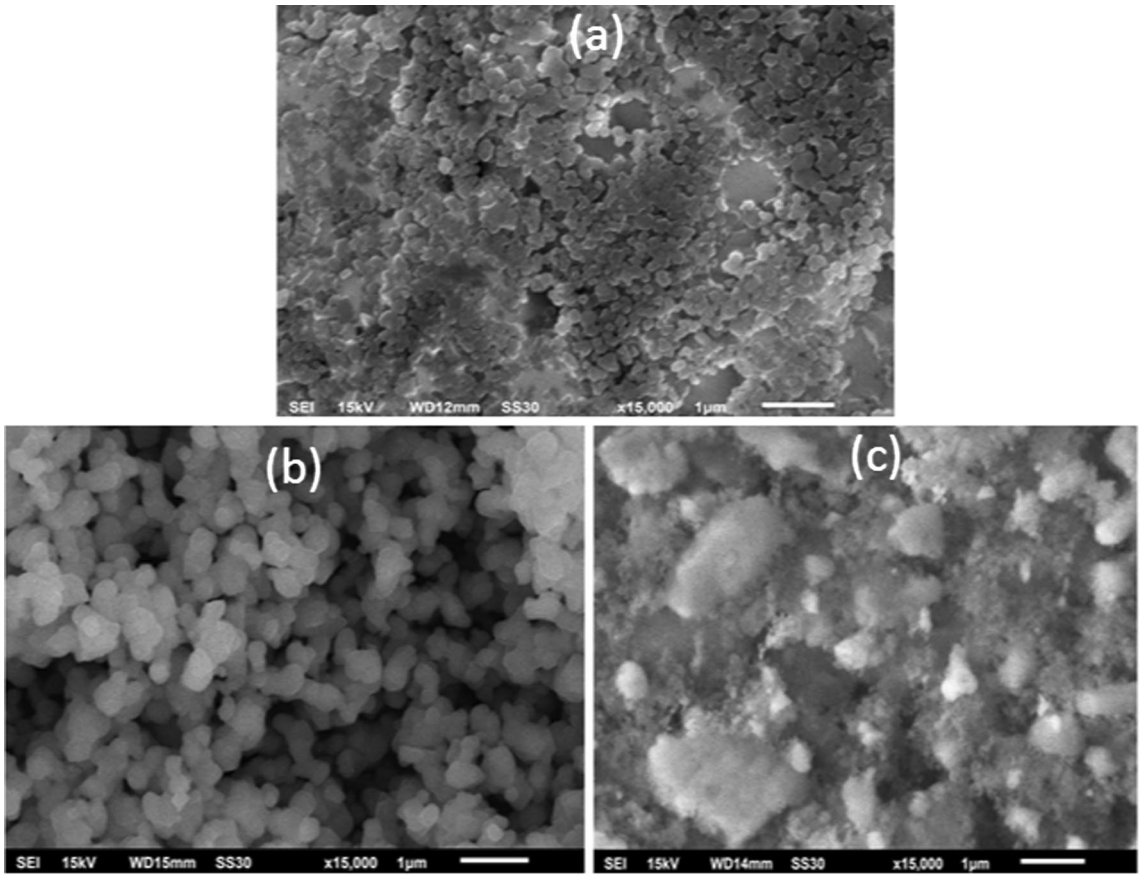

Fig. 3 Scanning electron microscopy images of **a** pure KI **b** KI–Al_2O_3 and **c** KI–TiO_2 composites

is called the space-charge layer which firmly modifies the bulk properties of the host material (ionic salt) [34, 35]. It is also evident that little density and enormous pores are available in the composite samples owing to the two-phase nature of the composites and the particle size difference between the host material and the added dispersoid. The image of KI−TiO_2 composite depicted in Fig. 3c displays that both the phases were present separately in the composite and demonstrating the firm interface–interface interaction. This interface–interface interaction produced the space-charge layer, responsible for the conductivity enhancement in the composite [36].

The average crystallite size was calculated by applying the Debye–Scherrer equation on KI at $2\theta = 24.9°$ (111 diffraction peak) by the following formula:

$$D = 0.89\lambda/\beta\cos\theta \tag{1}$$

D is the crystallite size, λ is the X-ray wavelength (1.5 Å), β is the full width at half maximum, and θ is the diffraction angle. Results show a gradual decrease in crystallite size from pure KI to KI–Al_2O_3 and KI–TiO_2 composites which confirms that incorporation of Ti and Al inhibits crystal growth of KI. This anomaly is probably due to the occurrence of Al−O−K and Ti−O−K linkage in the binary composites. Figure 3a shows large aggregated particles present in the crystal lattice which decreases upon the addition of alumina (Fig. 3b) and titania (Fig. 3c) which could provide intimate contact between them inhibiting the growth of crystalline KI. The crystallite sizes obtained were 15.85 nm (KI), 9.53 nm (KI–Al_2O_3), and 11.19 nm (KI–TiO_2).

Electrical conductivity

Impedance spectroscopy

AC impedance spectroscopic analysis has been an effective weapon for the examination of ionic conductivity in solid composites. The complex impedance is illustrated by:

$$Z^* = Z' - jZ'' \tag{2}$$

$$Z^* = \frac{D}{\omega C}\frac{j}{\omega C} \tag{3}$$

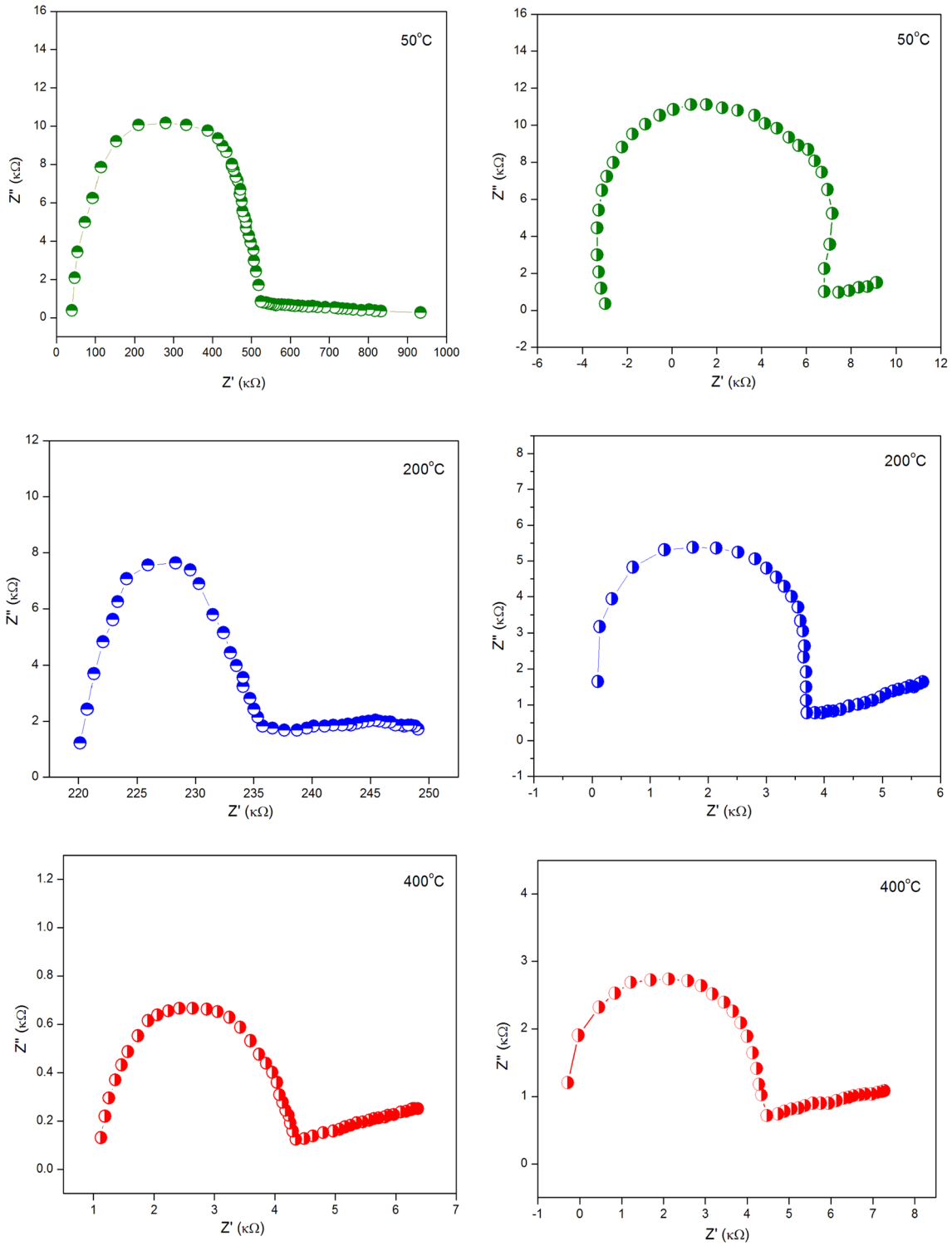

Fig. 4 Impedance spectra of **a** KI–Al_2O_3 and **b** KI–TiO_2 composites at 50 °C, 200 °C, and 400 °C temperatures

where Z' and Z'' is the real and imaginary part of impedance, respectively, ω is the angular frequency, C is the capacitance of the sample, j is the imaginary root of − 1 and D is the loss tangent. Figure 4a, b shows the Cole–Cole plot of KI−Al_2O_3 and KI−TiO_2 composites, respectively, at 50 °C, 200 °C, and 400 °C temperatures in the frequency range 20 Hz–1 MHz. The plots depict that there is a half-circular curvature at lower frequency region preceded by an inclined

straight line at higher frequency region as reported in our previous work [37, 38]. Plots of the imaginary part against the real part of complex impedance generate fine half-circles known as Cole–Cole plots and the center of the half-circles lies above the real impedance axis [36]. The impedance spectra of the composites present the apparent half-circle (Debye type relaxation of ions) together with a bulged out spike, as a result of the occurrence of the ionic polarization and electrochemical reaction at the electrode interface [39]. It is evident from the plots that the occurrence of only one half-circles at lower frequencies explains the simultaneous effect of both the grains and grain boundaries. The presence of the spikes in the spectra is the characteristic feature of composites with ionic conductivity [40]. Figure 4a, b shows that the impedance decreases with an increase in temperature. With an increase in temperature, the radius of the semicircle decreases attributing to the decrease in bulk resistance. Enhancement in crystalline nature with an increase in temperature could be the reason for the decrease in bulk resistance and an increase in ionic conductivity [41]. As we can see from Fig. 4 that at 400 °C of temperature KI−TiO_2 composite depicts slightly reduced semicircle as compared to KI−Al_2O_3 composite suggesting a slight decrease in bulk resistance and increase in ionic conductivity.

Ionic conductivity

The temperature-dependent electrical conductivity of the pure KI, KI−Al_2O_3, and KI−TiO_2 composites at a single frequency of 1 kHz is shown in Fig. 5. The conductivity of the composites follows the Arrhenius relation (Eq. 4):

$$\sigma_T = \sigma_0 \times e\left(\frac{-E_a}{kT}\right) \tag{4}$$

where σ_T is the total conductivity, σ_0 is the pre-exponential factor, E_a is the activation energy of ionic motion, and k is the Boltzmann constant. Figure 5 displays the temperature dependence of the ionic conductivity (Arrhenius plots) of the bulk part for the samples. After the dissolution of Al_2O_3 and TiO_2 ingredients into the matrix of KI heterogeneously, the ionic conductivity of the composites was improved. Two factors are responsible for the conductivity improvement on the incorporation of the amount of dispersoid Al_2O_3 and TiO_2 into the KI matrix 1. Grain boundary diffusion: This is the improvement in ionic conductivity within the interface area because at interface (disordered) area defect formation and migration enthalpies are prominently diminished. 2. Space-charge layers: The interface area promotes concentration profiles of point defects in the area adjacent to the disordered area in the ionic compound [42]. However, very little improvement is seen in the incorporation of Al_2O_3. The activation energies of conduction obtained from the data between 20−400 °C are tabulated in Table 1. As can be seen from the table, the activation energy of the pure KI slightly decreased upon adding the amount of Al_2O_3 and TiO_2 contents explaining the slight improvement in conductivity.

The ionic conductivity versus frequency ranging from 10 kHz to 1 MHz of pure KI, KI−Al_2O_3, and KI−TiO_2 samples at 30 °C is shown in Fig. 6. The AC conductivity of solid composites is reliant on the doping process and the structural deformations of composites [43, 44]. The highest conductivity for solid composites was attained at higher

Table 1 Activation energies calculated in the temperature range 20−400 °C

Sample	E_a (ev)
KI	0.23
KI–Al_2O_3	0.22
KI–TiO_2	0.21

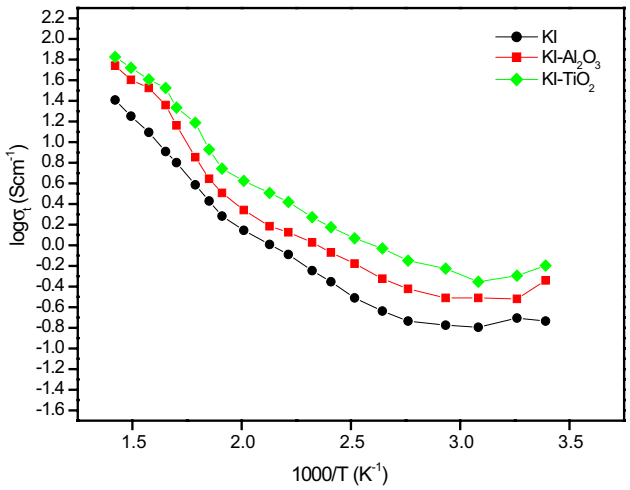

Fig. 5 Temperature-dependent ionic conductivity at 1 kHz

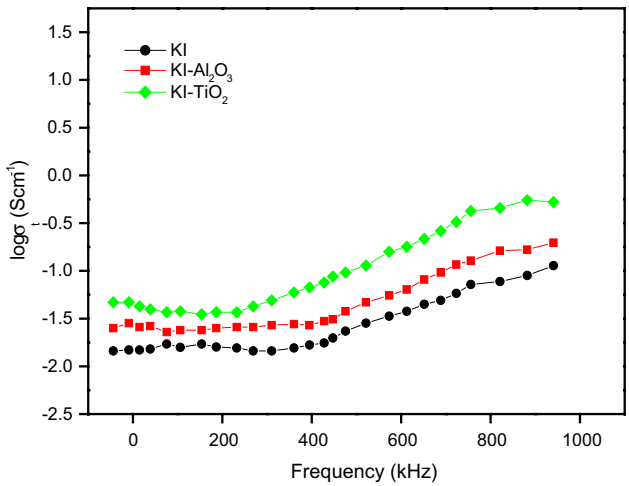

Fig. 6 Frequency-dependent ionic conductivity at 30 °C

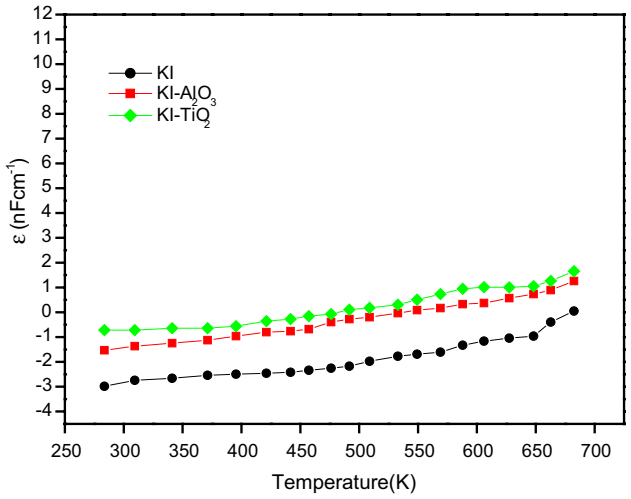

Fig. 7 Dielectric constant versus temperature at 1 kHz

frequency as depicted in the figure and also KI−Al_2O_3 and KI−TiO_2 has higher conductivity as compared to pure KI. This could result from small polaron hopping in the current composites [45]. At higher frequencies excitation is generated by the excited charges which increased in conductivity of KI−Al_2O_3 and KI−TiO_2 concerning the applied frequency [46, 47].

Dielectric study

Dielectric properties can be characterized as the amount of distortion (or polarization) of the organization of electric charge in the compound as a function of the frequency of the applied electric field. The dielectric constants of the solid samples can be calculated by:

$$\varepsilon = \frac{\mathrm{C}pt}{\varepsilon_0 A} \tag{5}$$

where Cp is the capacitance of specimen in Farad (F), t is the thickness of the pellet, ε_0 is the permittivity of free space (8.854×10^{-12} F m^{-1}) and A is the area of a flat surface of the pellet. Figure 7 compares variation of dielectric constant with the temperature at 1 kHz for the pure KI, KI−Al_2O_3, and KI−TiO_2 solid samples. It is evident from the figure that the dielectric constant increases with the increase in temperature in the complete temperature range examined which can be attributed to the mechanism of distortion of electric charges. At low-temperature range, active charges are at low energy state and therefore show less mobility which resulted in low contribution toward the distortion of electric charges and hence show diminished dielectric behavior. With the rise in temperature, the active charges become excited and have enough energy, consequently increasing the dielectric constant [48].

Conclusion

Electrical conductivity has improved, and activation energy of conduction has decreased slightly in the systems KI–Al_2O_3 and KI–TiO_2 compared to the pure KI. The highest ionic conductivity was observed in the ionic system KI–TiO_2. XRD and FTIR suggested the formation of solid composites between the host matrix (1st-phase) and the dispersoid (2nd-phase). The inputs obtained from the experiment suggesting significant ionic conductivity in the dispersed system owing to the establishment of space-charge layer between the 1st-phase and the second-phase in which defect formation increases and that is considered to be the authentic phenomenon of conductivity improvement. The compound is found to be in a two-phase system with Al_2O_3 and TiO_2 particles arranged between the particles of KI. The improvement of ionic conductivity in KI–Al_2O_3 and KI–TiO_2 in comparison with pure KI can be explained with the space-charge layer model. The improvement in conductivity is explained in terms of deformation mechanism at interface areas and space-charge layer formation in the bulk particles of KI.

Acknowledgements Authors are highly grateful to Aligarh Muslim University, Aligarh, for making available all mandatory research facilities. UGC is to be thanked for providing financial assistance. We also thank Jamia Millia Islamia, New Delhi, for XRD characterization.

References

1. Pirzada, B.M., Mir, N.A., Qutub, N., Mehraj, O., Sabir, S., Muneer, M.: Synthesis, characterization and optimization of photocatalytic activity of TiO_2/ZrO_2 nanocomposite heterostructures. Mater. Sci. Eng., B **193**, 137–145 (2015)
2. Shafi, A., Ahmad, N., Sultana, S., Sabir, S., Khan, M.Z.: Ag_2S-sensitized NiO – ZnO heterostructures with enhanced visible light photocatalytic activity and acetone sensing property. ACS Omega **4**, 12905–12918 (2019)
3. Wani, S.I.: Rafiuddin: synthesis, properties and application of titania incorporated potassium iodoplumbite nanocomposite solid electrolyte for the manufacture of high value capacitors. Electrochim. Acta **342**, 136097 (2020)
4. Zare, M., Solaymani, S., Shafiekhani, A., Kulesza, S., Talu, S., Bromowicz, M.: Evolution of rough-surface geometry and crystalline structures of aligned TiO_2 nanotubes for photoelectrochemical water splitting. Sci. Rep. **8**, 10870 (2018)
5. Sultana, S.: Rafiuddin: electrical conductivity in TlI-TiO_2 composite solid electrolyte. Phys. B Condens. Matter. **404**, 36–40 (2009)
6. Sultana, S., Rafiuddin, R.: Enhancement of ionic conductivity in the composite solid electrolyte system: TlI-Al_2O_3. Ionics **15**, 621–625 (2009)
7. Uvarov, N.F., Vaněk, P., Yuzyuk, Y.I., Železný, V., Studnička, V., Bokhonov, B.B., Dulepov, V.E., Petzelt, J.: Properties of

rubidium nitrate in ion-conducting $RbNO_3$–Al_2O_3 nanocomposites. Solid State Ion. **90**, 201–207 (1996)
8. Jander, W.: Neuere Forschungen über Diffusion und elektrische Leitfähigkeit fester Salze. Zeitschrift Für Angew. Chemie. **42**, 462–467 (1929)
9. Liang, C.C.: Conduction characteristics of the lithium iodide-aluminum oxide solid electrolytes. J. Electrochem. Soc. **120**, 1289 (1973)
10. Wagner, J.B.: Transport in compounds containing a dispersed second phase. Mater. Res. Bull. **15**, 1691–1701 (1980)
11. Wieczorek, W.: Entropy effects on conductivity of the blend-based and composite polymer solid electrolytes. Solid State Ion. **53–56**, 1064–1070 (1992)
12. Valverde-Diez, N., Wagner, J.B.: Electronic conduction in $AgI(Al_2O_3)$ composites. Solid State Ion. **34**, 175–179 (1989)
13. Tadanaga, K., Imai, K., Tatsumisago, M., Minami, T.: Preparation of AgI–Al_2O_3 composites with high ionic conductivity using Al_2O_3 aerogel and xerogel. J. Electrochem. Soc. **147**, 4061 (2000)
14. Shahi, K., Wagner, J.B.: Enhanced ionic conduction in dispersed solid electrolyte systems (DSES) and/or multiphase systems: Agl–Al_2O_3, Agl–SiO_2, Agl–Fly ash, and Agl–AgBr. J. Solid State Chem. **42**, 107–119 (1982)
15. Wagner, C.: The electrical conductivity of semi-conductors involving inclusions of another phase. J. Phys. Chem. Solids **33**, 1051–1059 (1972)
16. Takahashi, T., Teaneck, N.J., Wagner Jr., J.B.: High conductivity solid ionic conductors: recent trends and applications. World Scientific, Singapore (1989)
17. Mhiri, T., Colomban, P.: Defect-induced smoothing of the superionic phase transition in $Cs_{1-X}M_XHSO_4$ protonic conductors. III. Rubidium substitution. Solid State Ion. **44**, 235–243 (1991)
18. Uvarov, N.F., Isupov, V.P., Sharma, V., Shukla, A.K.: Effect of morphology and particle size on the ionic conductivities of composite solid electrolytes. Solid State Ion. **51**, 41–52 (1992)
19. Uvarov, N.F., Bokhonov, B.B., Isupov, V.P., Hairetdinov, E.F.: Nanocomposite ionic conductors in the Li_2SO_4–$A1_2O_3$ system. Solid State Ion. **74**, 15–27 (1994)
20. Maier, J.: Space charge regions in solid two-phase systems and their conduction contribution-I. Conductance enhancement in the system ionic conductor-'inert' phase and application on AgC1:$A1_2O_3$, and AgCl:SiO_2. J. Phys. Chem. Solids **46**, 309–320 (1985)
21. Huang, J., Bartell, L.S.: Structure and properties of potassium iodide nanoparticles. A molecular dynamics study. J. Mol. Struct. **567–568**, 145–156 (2001)
22. Noor, M.M., Buraidah, M.H., Yusuf, S.N.F., Careem, M.A., Majid, S.R., Arof, A.K.: Performance of dye-sensitized solar cells with (PVDF-HFP)-KI-EC-PC electrolyte and different dye materials. Int. J. Photoenergy **2011**, 1–5 (2011)
23. Aziz, M.F., Noor, I.M., Sahraoui, B., Arof, A.K.: Dye-sensitized solar cells with PVA–KI–EC–PC gel electrolytes. Opt. Quantum Electron. **46**, 133–141 (2014)
24. Achour, A., Islam, M., Solaymani, S., Vizireanu, S., Saeed, K., Dinescu, G.: Influence of plasma functionalization treatment and gold nanoparticles on surface chemistry and wettability of reactive-sputtered TiO_2 thin films. Appl. Surf. Sci. **458**, 678–685 (2018)
25. Sultana, S.: Rafiuddin: behaviour of electrical conductivity in CsI–Al_2O_3 and CsI–TiO_2 systems. Arab. J. Chem. **9**, S170–S176 (2016)
26. Yu, D.H., Yu, X., Wang, C., Liu, X.C., Xing, Y.: Synthesis of natural cellulose-templated TiO_2/Ag nanosponge composites and photocatalytic properties. ACS Appl. Mater. Interfaces. **4**, 2781–2787 (2012)
27. Nie, A., Yang, H., Li, Q., Fan, X., Qiu, F., Zhang, X.: Catalytic oxidation of chlorobenzene over V_2O_5/TiO_2–carbon nanotubes composites. Ind. Eng. Chem. Res. **50**, 9944–9948 (2011)
28. Rao, M.V.M., Reddy, S.N., Chary, A.S.: DC ionic conductivity of NaNO3: γ-Al_2O_3 composite solid electrolyte system. Phys. B: Condens. Matter **362**, 193–198 (2005)
29. Nadimicherla, R., Kalla, R., Muchakayala, R., Guo, X.: Effects of potassium iodide (KI) on crystallinity, thermal stability, and electrical properties of polymer blend electrolytes (PVC/PEO:KI). Solid State Ion. **278**, 260–267 (2015)
30. Ramesh, S., Sominska, E., Cina, B., Chaim, R., Gedanken, A.: Nanocrystalline γ-alumina synthesized by sonohydrolysis of alkoxide precursor in the presence of organic acids: structure and morphological properties. J. Am. Ceram. Soc. **94**, 89–94 (2000)
31. Kan, Y., Wang, P., Li, Y., Cheng, Y.-B., Yan, D.: Low-temperature sintering of $Bi_4Ti_3O_{12}$ derived from a co-precipitation method. Mater. Lett. **56**, 910–914 (2002)
32. Zeeshan, N.: Rafiuddin: solid electrolytes based on $\{1-(x+y)\}$ ZrO_2-(x)MgO-(y)CaO ternary system: preparation, characterization, ionic conductivity, and dielectric properties. J. Adv. Res. **9**, 35–41 (2018)
33. Desvals, M.A., Knauth, P.: Study of two-phase mixtures copper (I) bromide-alumina by impedance spectroscopy. J. Phys. Chem. Solids **58**, 319–324 (1997)
34. Uvarov, N.F., Vaněk, P.: Stabilization of new phases in ion-conducting nanocomposites. J. Mater. Synth. Process. **8**, 319–326 (2000)
35. Dygas, J.R., Malys, M., Krok, F., Wrobel, W., Kozanecka, A., Abrahams, I.: Polycrystalline BIMGVOX.13 studied by impedance spectroscopy. Solid State Ion. **176**, 2085–2093 (2005)
36. Iqbal, M.Z.: Rafiuddin: preparation, characterization, electrical and dielectric properties of $(1-x)$ (PbI_2–Ag_2CrO_4)–xTiO_2 composite solid electrolytes. Ceram. Int. **41**, 13650–13657 (2015)
37. Wani, S.I., Rafiuddin, R.: Impedance spectroscopy and conductivity studies of KCl-doped solid electrolyte. J. Theor. Appl. Phys. **12**, 141–146 (2018)
38. Wani, S.I.: Rafiuddin: structural, thermal, and electrical behavior of Cu-substituted $KPbI_3$ ternary compound. Russ. J. Phy. Chem. A **92**, 2811–2816 (2018)
39. Wu, M.-S., Hsieh, H.-H.: Nickel oxide/hydroxide nanoplatelets synthesized by chemical precipitation for electrochemical capacitors. Electrochim. Acta **53**, 3427–3435 (2008)
40. Onwudiwe, D.C., Arfin, T., Strydom, C.A.: Fe(II) and Fe(III) complexes of N-ethyl-N-phenyl dithiocarbamate: electrical conductivity studies and thermal properties. Electrochim. Acta **127**, 283–289 (2014)
41. Thambidurai, M., Muthukumarasamy, N., Velauthapillai, D., Agilan, S., Balasundaraprabhu, R.: Impedance spectroscopy and dielectric properties of cobalt doped CdS nanoparticles. Powder Technol. **217**, 1–6 (2012)
42. Knauth, P.: Ionic conductor composites: theory and materials. J. Electroceram. **5**, 111–125 (2000)
43. Pandey, K., Dwivedi, M.M., Singh, M., Agrawal, S.L.: Studies of dielectric relaxation and a.c. conductivity in $[(100-x)$ PEO + xNH4SCN]: Al–Zn ferrite nano composite polymer electrolyte. J. Poly. Res. **17**, 127–133 (2010)
44. Haldar, I., Biswas, M., Nayak, A.: Preparation and evaluation of microstructure, dielectric and conductivity (ac/dc) characteristics of a polyaniline/poly N-vinyl carbazole/Fe_3O_4 nanocomposite. J. Polym. Res. **19**, 9951–9959 (2012)
45. Gabal, M.A., Al Angari, Y.M.: Effect of diamagnetic substitution on the structural, magnetic and electrical properties of $NiFe_2O_4$. Mater. Chem. Phys. **115**, 578–584 (2009)
46. El Ghanem, H.M., Abdul Jawad, S., Al-Saleh, H.M., Hussain, Y.A., Salah, W.: Effect of dc-bias on the dielectric behavior of

CNT/ABS nanocomposites. Phys. B Condens. Matter. **418**, 41–46 (2013)
47. Godselahi, T., Vesaghi, M.A., Gelali, A., Zahrabi, H., Solaymani, S.: Morphology, optical and electrical properties of Cu–Ni nanoparticles in a-C: H prepared by co-deposition of RF-sputtering and RF-PECVD. Appl. Surf. Sci. **258**(2), 727–731 (2011)
48. Ahmed, R., Moslehuddin, A.S.M., Mahmood, Z.H., Hossain, A.K.M.A.: Weak ferromagnetism and temperature dependent dielectric properties of $Zn_{0.9}Ni_{0.1}O$ diluted magnetic semiconductor. Mater. Res. Bull. **63**, 32–40 (2015)